Applied Computing and Geosciences 8 (2020) 100042

Contents lists available at ScienceDirect

Applied Computing and Geosciences

journal homepage: www.journals.elsevier.com/applied-computing-and-geosciences

Animated visualization of post-glacial land uplift and shore displacement from modeled paleotopographic reconstructions

Viljami Perheentupa [a,*], Ville Mäkinen [a], Hando-Laur Habicht [b], Juha Oksanen [a]

[a] Finnish Geospatial Research Institute FGI, National Land Survey of Finland, Finland
[b] Department of Geoinformatics, Estonian Land Board, Estonia

ARTICLE INFO

Keywords:
Animated maps
Geovisualization
Land uplift
Shore displacement
Paleotopography
Glacial isostatic adjustment

ABSTRACT

Post-glacial land uplift and shore displacement are dynamic processes that are challenging to present with cartography and geovisualization. To communicate these phenomena, we have created a dynamic visualization in the form of high-quality animation, utilizing automated processes in the computation and rendering of large raster datasets. We have developed a simplified model to assess the past and future elevation models, and applied it to the High Coast/Kvarken Archipelago UNESCO World Heritage Site, which is considered one of the best places in the world to observe land uplift. Additionally, the ice decline in the area has been evaluated and visualized.

Based on the model and the present-day topography/bathymetry data, we provide a 40 fps 4K-resolution animation with an 80-s duration of the post-glacial history at the World Heritage Site and its vicinity, extending from 10,500 years ago to 1000 years in the future. Although they do not aim to contain the precision of thorough paleogeographic reconstructions, we have found that the individual frames of the animation are closely aligned with comparable geological data. We also present the computational process flow and the visualization principles used in the automated rendering, and thus aim to contribute to the cartographic presentation of geodynamic processes.

1. Introduction

Glacial isostatic adjustment (GIA) is an ongoing geodynamic process at the High Coast, Sweden/Kvarken Archipelago, Finland, UNESCO World Heritage Site. GIA is exhibited as land uplift, because Earth's crust, which was depressed by the continental ice sheet during the last glacial period, is rebounding towards the isostatic equilibrium. The maximum rate of absolute uplift in the area is about 10 mm per annum, and the maximum rate of apparent uplift, i.e. the uplift relative to the sea level, is almost 9 mm (Poutanen and Steffen, 2015). The area's coasts are separated by a marine region, the Gulf of Bothnia, which makes shore displacement an integral part of the uplift phenomenon. The Outstanding Universal Value (OUV) of the site is based on two main factors defined by UNESCO. First, both the High Coast and the Kvarken Archipelago show some of the highest rates of post-glacial uplift in the world, acting as key areas for the understanding of crustal response to the deglaciation. Second, the Kvarken Archipelago provides a unique view of the glacial depositional formations, and together the areas provide a representative example of a landscape shaped by post-glacial land uplift (UNESCO, 2006).

The cartographic representation of land uplift and shore displacement is often implemented in multiple small static maps with isobases representing the current land uplift rates or the current elevations of the ancient shorelines. These maps can contain a considerable amount of information in a single view but may fail to communicate the continuous nature of the phenomena to larger audiences. Furthermore, the gradual deceleration of land uplift cannot be efficiently shown in a static map presentation, and the actual displacement of shorelines is not visible. To create a dynamic visualization of the post-glacial history of the region, our aim is to produce an animated map in which the individual frames represent digital elevation models (DEMs) and shoreline reconstructions at given moments. Animated geographic time series are well established in the field of cartography (DiBiase et al., 1992) and can provide an optimal way of presenting data, because the human eye-brain system is particularly good at monitoring continuous movement (Dorling, 1992).

To calculate the DEMs required by the animation, we need to derive a mathematical model to estimate the topographic changes for more than 10,000 years in the past, since the period of deglaciation. Furthermore, to achieve the impression of continuousness using the common video standards with frame rates between 25 and 60 fps, an automated process

* Corresponding author.
E-mail address: viljami.perheentupa@live.fi (V. Perheentupa).

https://doi.org/10.1016/j.acags.2020.100042
Received 25 June 2020; Received in revised form 2 October 2020; Accepted 4 November 2020
Available online 7 November 2020

is required to produce and handle the thousands of frames that the animation contains.

Input data for the DEM reconstructions can be sought from the shoreline isobases at the different developmental stages of the Baltic Sea that have been created for Fennoscandia as a whole, e.g. by Eronen and Haila (1992), Eronen (2005), and Ojala et al. (2013). Eronen (2005) reconstructed the isobases for all the developmental stages of the Baltic Sea: the Baltic Ice Lake; the Yoldia Sea; the Ancylus Lake; and the Litorina Sea. The height interval of the isobases was 40 m for the Ancylus Lake, and 10 m for the Litorina Sea, which are the two partially or completely ice-free stages in our study area. These previous reconstructions were also utilized in the creation of the Ancient Shoreline Database (ASD) by Ojala et al. (2013), which serves as the state-of-the-art database of ancient shoreline site records in Finland. Furthermore, reconstructions estimating the actual ancient shorelines and not only their isobases have been made in Finland, e.g. by Tikkanen and Oksanen (2002) and the Geological Survey of Finland (GTK), and in Sweden by the Geological Survey of Sweden (SGU).

Some previous DEM reconstructions have also been made based on the shoreline isobases. Leverington et al. (2002) constructed a paleogeographic DEM of the Canadian Arctic by creating a raster surface interpolated from isobases and subtracting the result from the present-day DEM. Michael Lewis et al. (2005) created paleotopographic maps in the Great Lake region by fitting an exponential relaxation curve to ancient shoreline isobases, which provides the possibility of mathematically assessing the isostatic response of an area at a given time in the past. Mäkiaho (2009) performed a similar analysis for the Helsinki region in Finland, interpolating between timesteps and thus creating reconstructions for multiple moments. Other examples of DEM reconstructions are those of Rosentau et al. (2011), and more recently, Muru et al. (2018) and Nirgi et al. (2019). However, with the computational power of today's high-performance computing (HPC) clusters, we have no practical limitations in computing and rendering thousands of high-resolution DEMs, and creating a continuous time series that can be displayed as an animation. To our knowledge, a similar process has only been implemented before with the animated visualization of shore displacement in North Ostrobothnia by Oksanen (2012), and no systematic description of such a process has been published.

Although the technical feasibility places no restrictions, challenges exist in the development of a modeling approach, harmonizing the input data, and the dynamic visualization. The shoreline isobase reconstructions covering the study area only give dated isobases for two post-glacial phases at the Ancylus Lake and Litorina Sea development stages. Together with these reconstructions, we have the present-day DEM and the present-day land uplift rates to use as input data for the model. To the best of our knowledge, there is no established method to compute a given DEM reconstruction in between these known data points, and achieving this requires applying the information about the post-glacial relaxation of the crust derived from the previous geological studies.

Secondly, there is no uniform topographic/bathymetric model readily available with sufficient resolution for the whole study area. LiDAR-derived DEMs for both Finland and Sweden exist, but have been sampled into different projections and spatial resolutions. Moreover, the bathymetric data between the coasts is coarse and mostly modeled instead of measured, and yet sampled in a projection different from either of the elevation models. Therefore, creating a uniform input dataset requires careful resampling, re-projection, and merging of the topographic and bathymetric raster data to avoid both computational and visual errors in the resulting reconstructions.

Finally, there are the challenges related to geovisualization and cartographic presentation. The same animation must be able to communicate not only the shore displacement but also the ongoing land uplift on the regions already free of water as well as on the regions still underwater. Also, the coasts of Finland and Sweden have very different topographic reliefs, and a balanced visualization between them will require compromises both with the vertical exaggeration of the topography and with the speed in which the animations proceeds. A cartographically sound result with these topographic data that show such dissimilar changes on different parts of the map over time, requires a lot of manual experimenting with the visualization parameters.

We introduce a simplified method for the creation of ancient and future elevation models based on current land uplift rates, present-day topography and bathymetry, and past shoreline isobases derived from the geological evidence. We present a process for computing and rendering the DEMs based on a mathematical model, and apply this to a study area where comparative static reconstructions are available. Finally, we produce a high-resolution animation of land uplift and shore displacement, and discuss the special requirements, challenges, and limitations the dynamic visualization introduces.

2. Data and modeling

2.1. Study area

The study area's core is located at the High Coast (63°04′N, 18°22′E, Sweden)/Kvarken Archipelago (63°16′N, 21°10′E, Finland) UNESCO World Heritage site. The area forms a joint World Heritage Site between the Swedish coast on the western side of the Gulf of Bothnia and the Finnish archipelago on the eastern side, and is considered one of the best places in the world to observe the effects of land uplift (Poutanen and Steffen, 2015). The coasts have very different elevation reliefs: The High Coast is characterized by steep shores and till-capped hills; the Kvarken Archipelago consists of low elevation islands and De Geer formations, gaining new land area significantly more quickly than the High Coast region (Fig. 1). The study area contains the entire World Heritage site and a relatively large area around it, the total area being about 68,000 square kilometers. The maximum rate of apparent land uplift in the study area is close to 9 mm/a, located near Umeå (Poutanen and Steffen, 2015; NKG2005LU), and the minimum rate is approximately 5.6 mm/a at the southeastern edge of the study area (NKG2005LU).

2.2. Data

The present-day topographic and bathymetric models were created based on the most recent LiDAR-derived DEMs of Finland and Sweden, and the HELCOM Baltic Sea Bathymetry Database (BSBD). Finland's elevation data were acquired from the National Land Survey of Finland (Maanmittauslaitos) as a raster with a pixel size of 2 m, EPSG:3067, in the N2000 height system. Sweden's elevation data were acquired from the National Land Survey of Sweden (Lantmäteriet) as a raster with a pixel size of 1 m, EPSG:3006, in the RH2000 height system. The rasters were re-projected onto an EPSG:3857 Pseudo-Mercator projection to facilitate any future use in web map applications and resampled into a 10-m spatial resolution. As the visualized area is only about 430 km from north to south, the use of this projection did not introduce further cartographic issues.

The BSBD consists of modeled bathymetry with a spatial pixel of 400 m, EPSG:3035. The data were re-projected onto the same coordinate system with the elevation data and oversampled into 10-m spatial resolution. As the data in the BSBD were non-existent or of weak quality close to the shorelines, we remodeled the data to create a plausible coastal bathymetry. This was done to enable the visualization of the future shore displacement estimations and was not considered to contain the precision of the terrestrial elevation models.

The elevation and bathymetric models were merged into a single raster, which was cropped and resampled into 4K (3840 × 2160) pixel dimensions. These dimensions were selected to optimize the resulting animation to the best and most widely available consumer-level screen resolutions, while avoiding unnecessary subpixel-level computations.

The land uplift model used was NKG2005LU, by the Nordic Geodetic Commission (NKG). The model shows the current uplift rates with a pixel

Fig. 1. Landscapes from the Skuleskogen National Park, High Coast, Sweden (a) and the Kvarken Archipelago, Finland (b). All the visible land areas in the images have risen above sea level due to land uplift. Photographs: Fabiola De Graaf, 2018.

size of approximately 1 km within the study area, and was resampled to the same resolution and projection with the elevation and bathymetric data to enable raster algebra between the different data layers. In this study, the land uplift rates are always used to refer to the apparent uplift, which is relevant in terms of shore displacement. By the time of the study, a newer land uplift model, NKG2016LU, was already available. However, the corrections in current height systems used in Finland and Sweden, N2000 and RH2000 respectively, are based on NKG2005LU. Furthermore, the effect of changes in land uplift rates and improvements in measurement precision in the last few years can be considered trivial for this purpose.

2.3. Deriving the ancient and future elevation models

A mathematical model was created to reconstruct the ancient and future elevation models. The model was based on the previously created present-day topography/bathymetry model (hereafter referred to as DEM_0), the NKG2005LU land uplift model with the current annual uplift rates, and the isobases of the ancient shorelines of the Ancylus Lake and the Litorina Sea as reported by Eronen (2005).

We determined the correlation between the shoreline isobases and the current uplift rates by investigating the uplift values in several locations scattered along the isobases. For both the Ancylus and Litorina stages, we found a near-linear correlation between the current uplift rates and the current elevations of the ancient shorelines (Fig. 2), as we had expected. We therefore constructed a linear model between the current uplift rates and the shoreline elevations (Eq. (1)). We used the shorelines' radiocarbon dating from Eronen (2005) and converted these dates into calendar years (cal yr), using the CalPal2007_HULU calibration curve (Danzeglocke et al., 2008). We then applied the linear model to evaluate the total uplift for the last 10,500 years (nominally 10,458 years, as derived from the calibration). From the linear regression between the current elevations of the 10,500 cal yr BP shorelines and the current land uplift rates, we obtained:

$$U_0 = 72.594 \frac{m \cdot a}{mm} u - 284.319\ m, \tag{1}$$

where U_0 is the elevation difference (m a.s.l.) between 10,500 cal yr BP and DEM_0, i.e. the total land uplift until the present, and u is the current land uplift rate in millimeters per year.

The exponential relaxation curve of GIA is well established in Fennoscandia (e.g. Linden et al., 2008; Nordman et al., 2015; Ekman, 2017), and it is caused by the relieving pressure as the depressed crust moves closer to the isostatic equilibrium. We therefore applied an exponential model (Eq. (2)) between the shoreline elevations of the recent past and those of the Ancylus (ca. 10,500 cal yr BP) and Litorina (ca. 8000 cal yr BP) stages (Fig. 3). To make the model more robust close to the present day, we applied the formula introduced by Ekman (2001), with the current uplift rates assumed constant for the last 1200 years. At this point, we excluded the assumed annual sea level rise of 1 mm presented in the formula, because this was not related to the relaxation of the crustal rebound.

We chose to base the relaxation curve on the uplift rate of 7 mm/a, as this closely represented the prevailing uplift rate in the core area. We also tested the formula with different fixed uplift rates between 5 and 9 mm/a and concluded that the non-linear patterns of relaxation were very similar, regardless of the nominal uplift rate, i.e. a single relaxation curve was sufficient to evaluate the decay of land uplift in the entire study area. We adapted the formula of exponential relaxation by Walcott (1980) from Nordman et al. (2015) and applied it as:

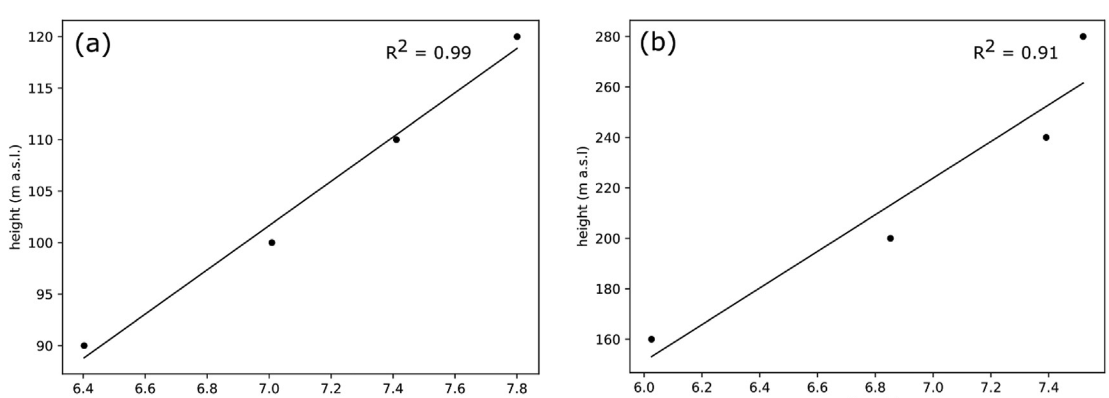

Fig. 2. Linear regression between ancient shoreline isobases and current annual land uplift rates. Litorina Sea stage ca. 8000 cal yr BP (a) and Ancylus Lake stage ca. 10,500 cal yr BP (b). The points represent the average annual uplift rate along the isobase.

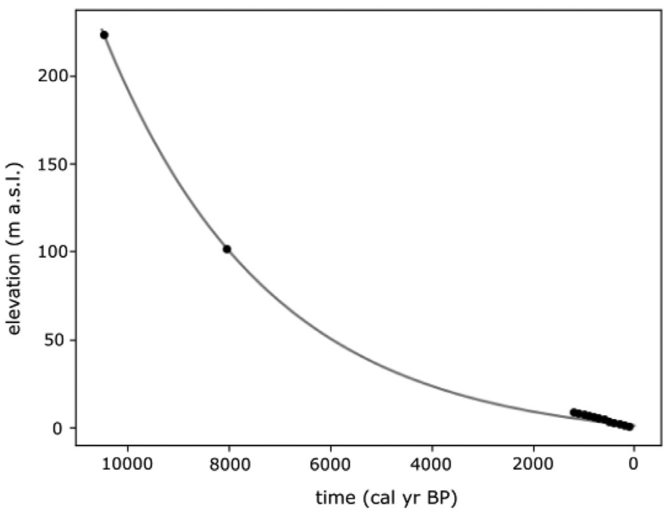

Fig. 3. A graphical representation of Eq. (2). The points at ca. 8000 and 10,500 cal yr BP have been calibrated based on the shoreline isobases of the Ancylus and Litorina stages according to Eronen (2005).

$$h(t) = a\left(e^{\frac{t}{b}} - 1\right) + c, \tag{2}$$

where h is the sea level elevation (mm a.s.l.), t is time (cal yr BP) and the constants are $a = 9400$ mm, $b = 3262$ yr, *and* $c = 740$ mm. These constants were derived from the exponential fit of the data displayed in Fig. 3.

Eq. (2) was used to create a scale factor for U_0 between the present day and 10,500 cal yr BP to derive the DEM of a given year (DEM_t) by subtracting the land uplift since that year from DEM_0. The land uplift since t cal year BP can be defined as:

$$U_t = U_0 \frac{a\left(e^{\frac{t}{b}} - 1\right) + c}{a\left(e^{\frac{10458}{b}} - 1\right) + c}, \tag{3}$$

where $t > 200$ and the year 10,458 cal yr BP is the nominal year we obtained from the calibration of the Ancylus stage shoreline dating. The constants a, b and c are same as in Eq. (2).

Finally, we can calculate the elevation model of a given year as:

$$DEM_t = DEM_0 - U_t. \tag{4}$$

With DEMs closer than 200 years to the present, as well as with the future DEMs, we assumed that the current uplift rates remained practically constant during the following centuries in line with Poutanen and Steffen (2015).

The model did not consider the historical variations in the eustatic sea level, as the shoreline displacement curves showed no evidence of transgression phases where the sea level would have risen faster than the rate of land uplift in the area (Berglund, 2004; Påsse and Anderson, 2005). Similarly, we did not take into account the potential future sea level rise caused by human-driven climate change, because most of these climate models only extended to a very near geological future of less than 200 years, and the time range of this study was more than 10,000 years in the past to 1000 years in the future. Moreover, even the near-future sea level rise of the Baltic Sea cannot be directly derived from the global sea level rise, e.g. because of the changing gravity near the melting ice sheet (Johansson et al., 2012; Poutanen and Steffen, 2015), and the relative sea level decrease in the Gulf of Bothnia is nevertheless expected to continue in the future (Church et al., 2013; Johansson et al., 2012).

Finally, the elastic rebound that takes place directly after the deglaciation was not considered, and the declining ice sheet is included in the animation only to bring viewers to the correct context from the start.

3. The land uplift and shore displacement animation

3.1. Computation and visualization of the DEMs

The time range for the computation of the animation frames was set between 10,500 cal yr BP and 1000 years after the present to show the land uplift immediately after and concurrent with the deglaciation until the near geological future. In this context, the present moment refers to the approximate time when the datasets used were measured, which was fixed for simplicity to the year 2000. The computation of transformed DEMs was implemented as an automated Python process, utilizing GDAL and NumPy libraries for raster processing and algebra. The timestep was set to five years to enable a smooth and seamless transition between the animation frames. In the early frames, where the continental ice sheet was still present, the timestep was set to one year, because the ice decline happened very quickly compared to land uplift.

The DEMs were visualized using a programmatic conversion of raster files into RGB images. The visualization of shore displacement was implemented by a discontinuity in the sea level elevation-dependent color scale. The bathymetry was visualized with a continuous color scale in shades of blue until an elevation of zero meters. Elevations above zero were visualized with hypsometric tints, starting with green, to create an impression of a discrete shoreline (Fig. 4). The RGB conversion was also implemented as a Python process using Matplotlib and Python Imaging Library (PIL). Matplotlib was also used to create a relief shading for each image, which was blended with the image by multiplication using PIL.

The file size of each rendered DEM was 31.6 MB in Tagged Image File Format (TIFF). The processing was executed using the HPC clusters of the CSC – IT Center for Science, Ltd. (Espoo, Finland) provided by the Open Geospatial Information Infrastructure for Research (oGIIR, urn:nbn:fi:research-infras-2016072513). The addition of cartographic and auxiliary elements, such as place names and timestamps, was carried out with Mapnik as a Python-driven process. The process flow, from computing the DEMs to the final rendering of the frames, is presented in Fig. 5.

3.2. Assessing and visualizing the ice decline

The ice decline over the study area was estimated according to Stroeven et al. (2016), who evaluated the ice chronology of the Fennoscandian ice sheet based on several geological proxies. The study's supplementary material was used to determine the ice margins with an interval of a hundred years over the study area. The estimated annual ice margins were calculated by interpolating a raster surface from these line features, in which each cell possesses an estimated value of the deglaciation year, and by creating new contour lines from this surface with a one-year timestep. This resulted in smoother ice margin lines than a direct interpolation from the original lines and produced a smoother visualization in terms of the animation.

The ice sheet was visualized by imitating real continental ice. This was done by using the DEM of Antarctica by the Polar Geospatial Center (Howat et al., 2019). A fully glaciated area roughly corresponding to the size of our study area was selected from the DEM and visualized with simple adjustments in brightness, contrast, and color scale to create a visual impression of the ice cover as viewed from above. The resulting image was processed to the extent of the annual ice margins, using GDAL and Shapely libraries. The edge of the ice sheet was visualized by creating a drop shadow for the line feature denoting the ice margin of a particular year.

3.3. Resulting animation

The final product of the process was a continuous animation of the post-glacial land uplift and shore displacement in the study area, including the deglaciation period. The animation was assembled using

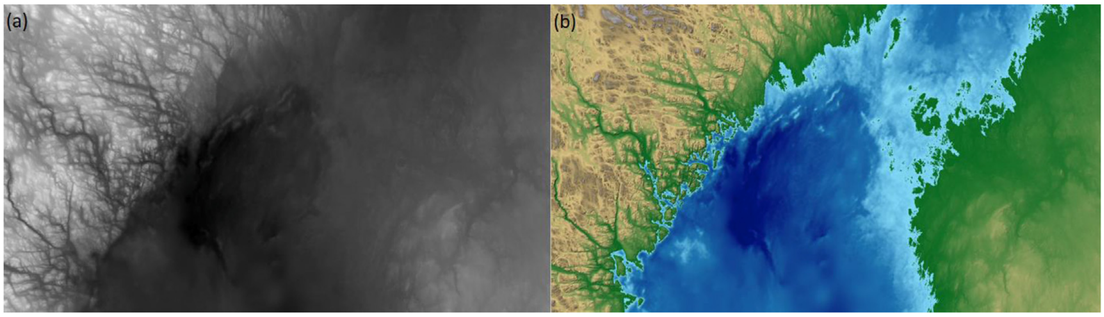

Fig. 4. DEM_0 in grayscale (a) and RGB-converted image, including relief shading of the same frame (b), where the impression of a discrete shoreline is created by a discontinuity in color scale between blue and green. (For interpretation of the references to color in this figure legend, the reader is referred to the Web version of this article.)

the Shotcut (Meltytech, LLC) open-source video editor. A suitable frame rate for the animation was evaluated, based on the visual balance between the opposite coasts and their shore displacement patterns. A balanced compromise was needed to present the horizontally rapid and steady shore displacement of the Finnish coast and the slower proceeding of the shorelines in Sweden, characterized, however, by abrupt isolation events. The gradual deceleration of the phenomenon also posed a challenge for dynamic visualization: considerably fewer changes would take place toward the end of the animation no matter which frame rate was used. Based on these requirements, the frame rate in the final animation was 40 fps, which meant the animation proceeded at 200 years per second in the post-glacial phase, and 40 years per second in the deglaciation phase. The frame rate of 40 fps also made it possible to view the animation in slower motion without losing the effect of continuousness. The full duration of the video at normal speed was 80 s, including the still frames of the present-day situation and at the end of the animation.

The animation presented two phenomena, post-glacial land uplift and the related shore displacement, with a spatial and temporal resolution that had not previously been achieved for a study area of this size. Land uplift was presented through the continuous change in the elevation-dependent color scale, both in terrestrial and submarine areas. Shore displacement was communicated through the discrete discontinuity between the submarine and terrestrial color palettes, which at the actual size of the animation created the effect of a sharp shoreline. In addition, the animation contained a set of place names to provide spatial context, a counter to show the year of reconstruction, and a dynamic timeline with a rotating wheel to indicate the time relative to the whole post-glacial history and the prevailing development stage of the Baltic Sea (Fig. 6).

As very little cartographic information other than the topography needed to be shown in the frames, rich colors and strong contrast were used in the visualization, while preserving the readability of the cartographic annotation. Examples of the frames are shown in Fig. 7, and the iterative visualization process is demonstrated in Fig. 8.

4. Discussion

4.1. Data quality and accuracy of the reconstructions

It was possible to attempt an evaluation of the model's precision by comparing the results with the previous reconstructions from the moments at which they were available. Our reconstructions are in agreement with the available shoreline reconstructions between 10,000 and 4000 cal yr BP of the Geological Survey of Sweden SGU (Fig. 9). Furthermore, the reconstructions of our study appeared to be visually in line with the Ancylus and Litorina stage shoreline reconstructions of Ojala et al. (2013) and Tikkanen and Oksanen (2002) on the Finnish side of the gulf, when the dating of those reconstructions were calibrated to calendar years. These comparisons gave encouraging results when evaluating the model and approach used in this study, although the production of completely accurate shoreline reconstructions for fixed moments was not the study's main focus.

The accuracy of both future and past reconstructions was ultimately limited due to the data quality. The original elevation models from Sweden and Finland represented high-quality data with more than sufficient spatial resolution for this purpose. The distortion caused by differences in height systems of N2000 (Finland) and RH2000 (Sweden) was maximally 2 mm at the Swedish-Finnish boundary, and the systems have been corrected for the post-glacial rebound with the same NKG2005LU model (Saaranen et al., 2009). However, the low quality of available bathymetric data was a restricting factor for the future shoreline estimations. The measurement and distribution of such data were restricted both technically and legally, and in the shallow coastal areas, which are the most interesting for the scope of this study, practically no data were available. Even in the areas where bathymetric data were available, the data were mostly modeled and not measured, and the spatial resolution was insufficient for a smooth visualization. The visualized future estimations therefore only represent the remodeled, interpolated surface, where the actual details of the seafloor are unknown.

Although the current DEMs are of high quality in accuracy and resolution, using the present-day topography as initial data poses some problems for reconstructions of the past. The features created after the land has emerged from the sea, both by natural processes and human interaction, are passed to the ancient reconstructions, and even at this scale level, can cause some notable artifacts. With this area and scale, the clearest distractions are caused by riverbeds that are sufficiently prevalent to place undesired features on the modeled ancient seafloor, distorting the land uplift and shore displacement chronology. These distractions are the most dominant on the Finnish side of the area. Sedimentation and biological processes such as peatland formation also affect the elevation models. If the spatial pixel were smaller, which might be the case with a smaller area of interest or with a zoom-enabled map application, the road network and other human-built environment would also introduce a problem.

The problems caused by the riverbeds could be eased by selective smoothing of the DEMs. However, some detail of the DEMs would be lost, and it was difficult to directly evaluate the extent to which the features were caused by post-glacial fluvial processes. We also tried placing the current stream network as a cartographic element over the problematic areas, but were dissatisfied with the visual result. Overall, these distractions were tolerable, given the animation's scale level.

Another issue for the accuracy is the dating uncertainties. In reality, the ancient shoreline isobases used in the modeling are not fixed to a single year or even to a single century, but describe an era of some hundreds of years. Finally, even the present-day topographic/bathymetric model is slightly asynchronous, depending on the data acquisition time, although this effect can be considered negligible.

It is also to be noticed that the elastic rebound, which has a significant role right after the deglaciation, was not taken into account in the computational model. When we observe the correlations shown in Fig. 2, we see that the consistency between present uplift rates and the shoreline

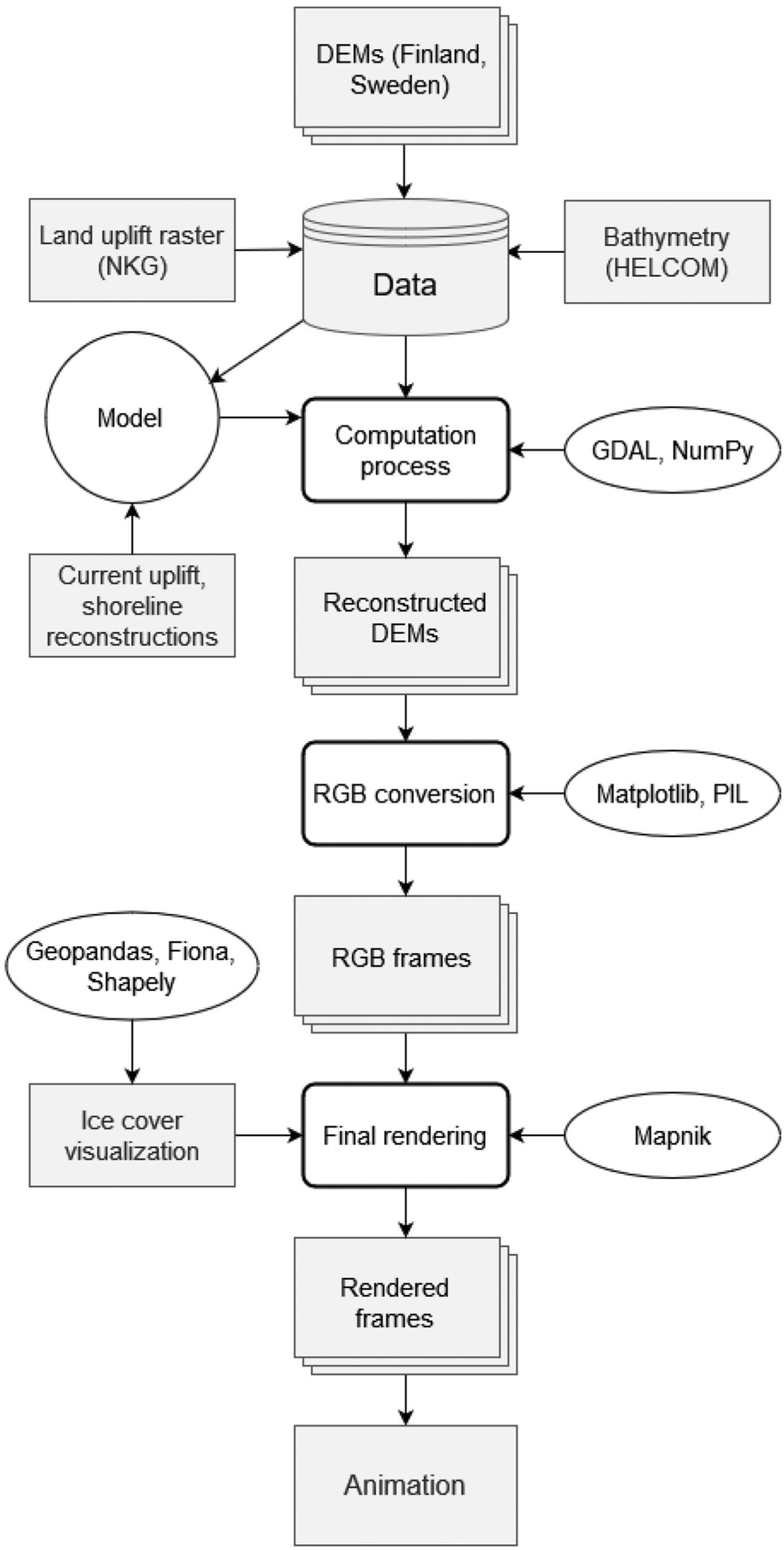

Fig. 5. The simplified process flow for producing the land uplift animation, using Python. The essential Python modules required are specified for each step in the process.

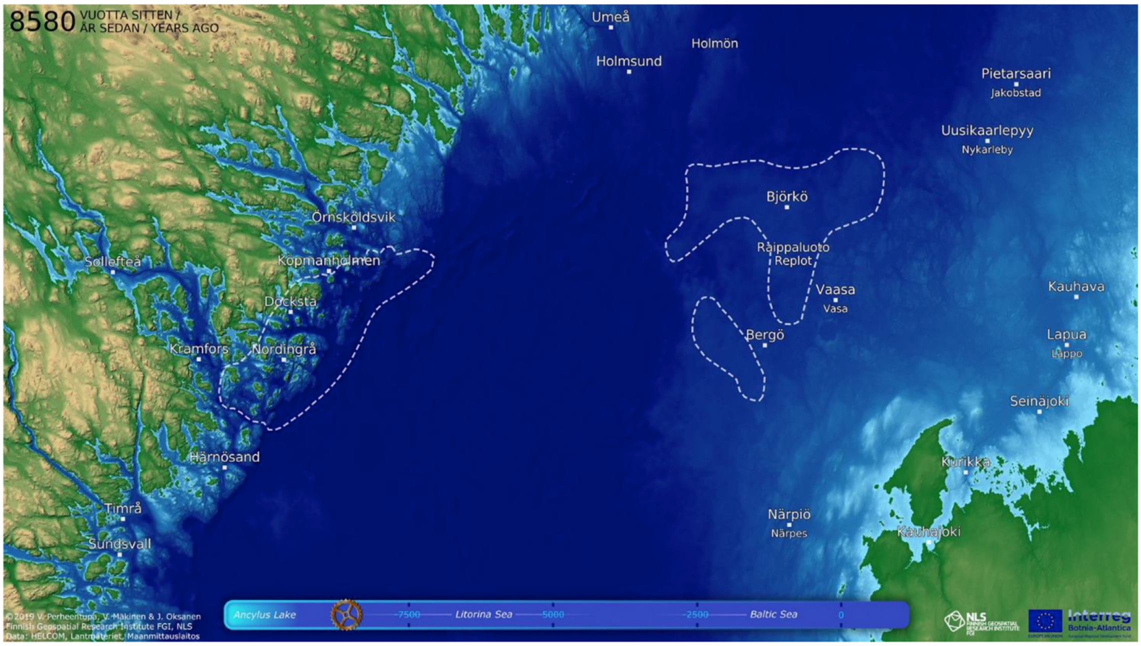

Fig. 6. A screen capture from the animation, illustrating a scene at 8580 cal yr BP, with all the cartographic and auxiliary elements, including the borders of the World Heritage Site and the dynamic timeline.

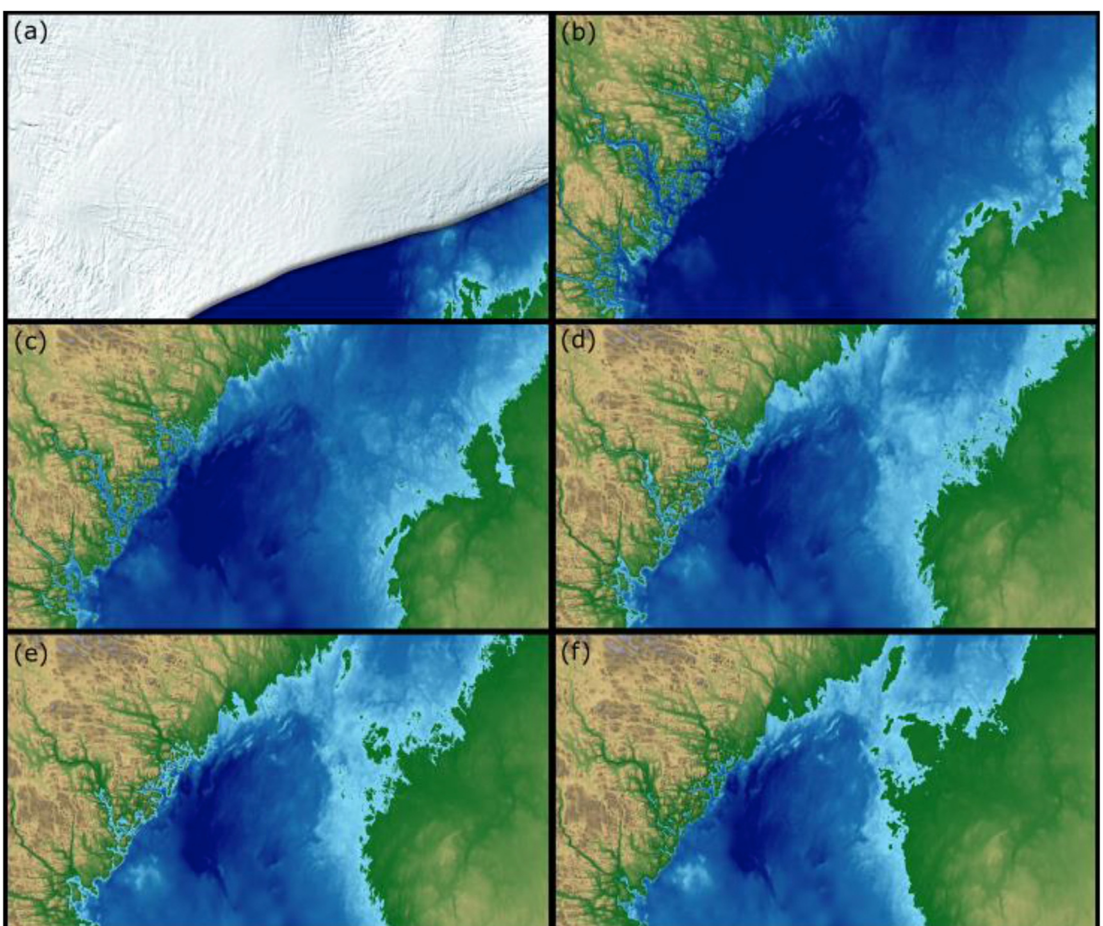

Fig. 7. Samples of individual image frames used to construct the animation. The images show the study area at 10,500 (a), 7500 (b), 5000 (c), and 2500 cal yr BP (d), the present stage (e), and the estimation after 1000 years (f). For readability, the cartographic elements and annotation are not included.

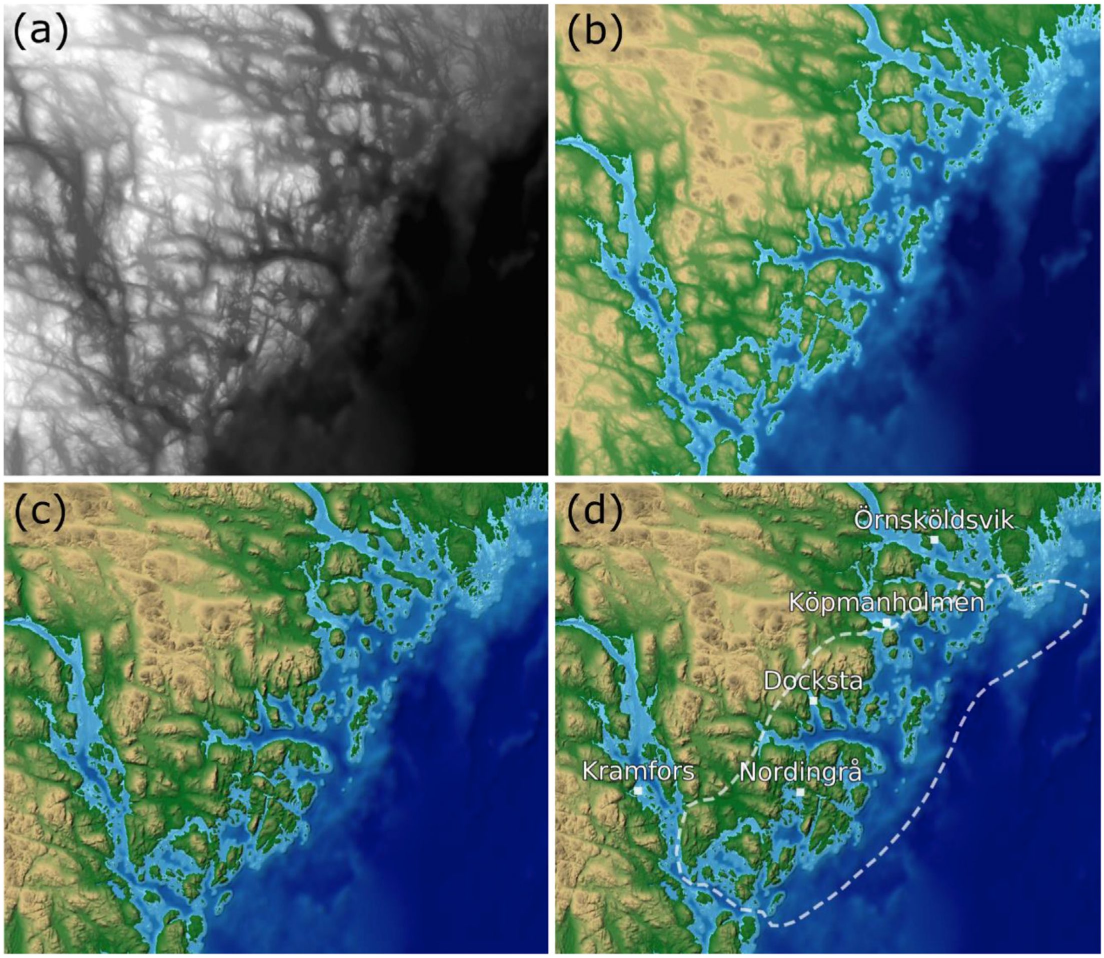

Fig. 8. Visualization phases of topographic data shown at the High Coast area, Sweden. Raw DEM in grayscale at 4000 cal yr BP (a), DEM assigned with elevation-dependent color scale (b), relief shading blended to the images with multiplication (c), and other cartographic elements overlaid on the image (d). (For interpretation of the references to color in this figure legend, the reader is referred to the Web version of this article.)

isobases is not as good with the Ancylus stage as it is with the Litorina stage, and the highest isobase appears as an outlier. If this isobase is disregarded, we reach a coefficient of determination similar to the Litorina stage ($R^2 = 0.99$). It is possible that the elastic rebound accounts for this inconsistency and not taking it into account has an impact on the model as a whole. This highlights that the computational model could certainly be improved by including more geophysical and geodynamic modeling. Omitting the elastic rebound in the modeling also results in the animated visualization not presenting this phenomenon and, therefore, the visualization could also be improved by taking it into account.

4.2. Future insights

The presentation of the animation could be further improved by providing the animation as a web map application with zoom and navigation functionalities. An animated map with a zoom function would require a smaller spatial pixel, and this poses a challenge with current video resolutions. For example, using the 10-m spatial resolution of the original resampled DEMs would exceed the dimensions supported by regular video formats. The animation would also ideally need to work on an existing web map platform, which may create even stricter conditions. A potential way to provide the animation with those pixel dimensions would be to utilize the time dimension support in the Web Map Service (WMS) protocol and fetch the timestamped map tiles, using e.g. the TimeDimension utility of the Leaflet JavaScript library. An alternative approach might be to process the DEMs in smaller tiles and produce separate animations from each set of tiles, and to present all the resulting animations simultaneously over a map. Either way, an interactive map application with more functionalities would provide significant extra value to the presentation of the animation.

Future research could also include the application of the method described to a larger geographical area. However, this would introduce new challenges, because the shore displacement curves are not as straightforward in many regions of Fennoscandia, because they include transgression phases. The ice-dammed lakes would also need to be considered.

5. Conclusions

The land uplift and shore displacement animation created as a result of this study provides a novel way to dynamically present the extraordinary post-glacial history of the High Coast/Kvarken Archipelago UNESCO World Heritage Site. The study introduces a method and process to achieve the same for any area affected by these phenomena, as long as the local attributes, such as local shore-level chronologies and displacement curves, are accounted for in the modeling. The study also provides guidance and visual examples that may prove helpful in the dynamic visualization of topographic data.

The reconstructions created in this study display good coherence with previous shoreline reconstructions where available. The future shoreline

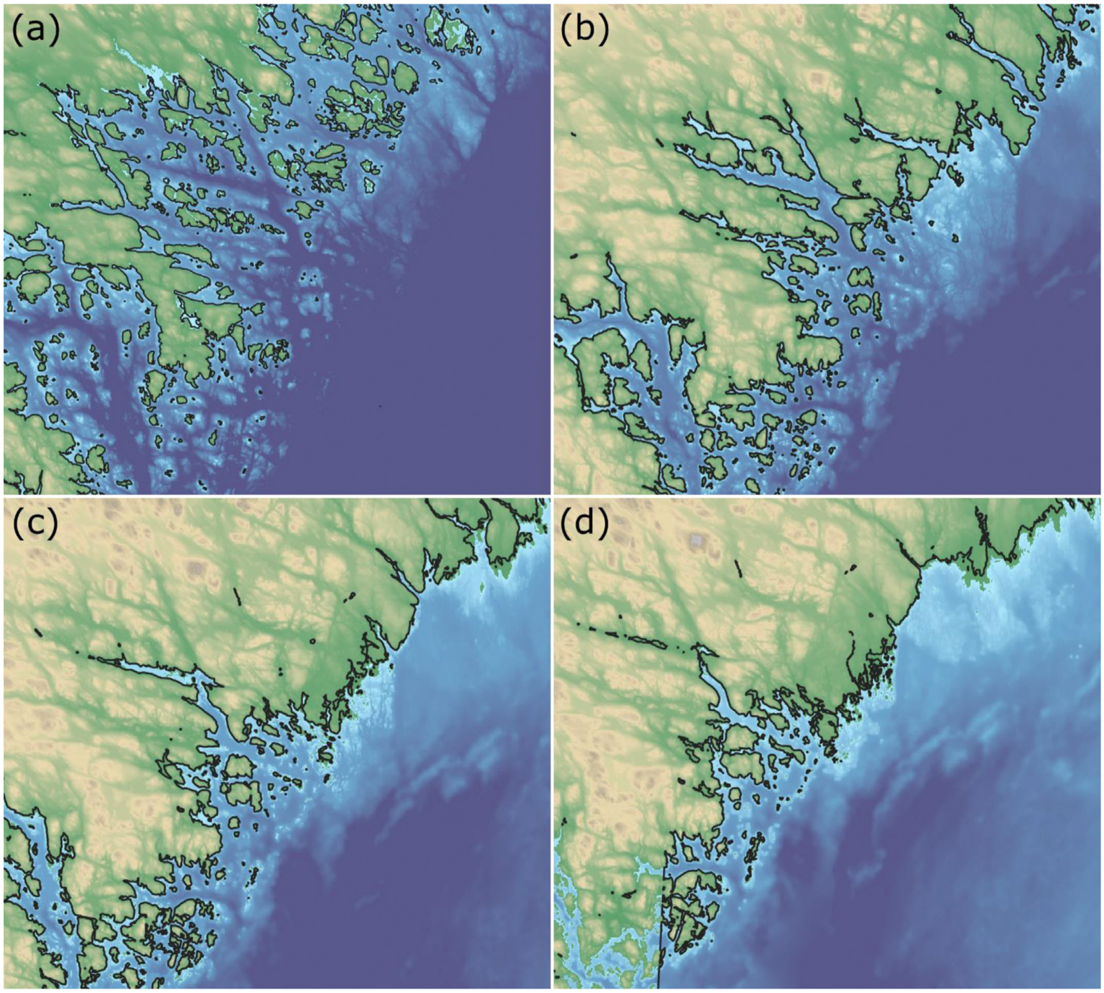

Fig. 9. Comparison between shoreline reconstructions of SGU (black line) and shorelines derived from the model of this study at the Swedish coast. Comparison shows reconstructions at 10,000 (a), 8000 (b), 6000 (c), and 4000 (d) cal yr BP.

estimations are uncertain because of the limited quality of the bathymetric data and the uncertainties in the future development of the Baltic Sea surface level. In addition to improvements in data and modeling, the overall presentation could be further developed by creating a map application with interactive functionalities from higher-resolution DEMs. Applying the method to a larger geographical area could also be considered.

Data availability

The essential computer code used in the creation of the reconstructions and the animation frames can be found at:

https://github.com/LystraFGI/LystraSourceCode.

The animation can be viewed at:

www.youtube.com/watch?v=TpwfCDlo7jg.

The dataset including the elevation data of Sweden is not to be made public according to the license agreement between the authors and the data provider.

Credit author statement

Viljami Perheentupa: Writing - original draft, Writing - review & editing, Methodology, Visualization, Software, Ville Mäkinen: Writing - review & editing, Methodology, Hando-Laur Habicht: Writing - review & editing, Formal analysis, Juha Oksanen: Writing - review & editing, Conceptualization, Methodology, Funding acquisition.

Authorship statement

Viljami Perheentupa implemented the modeling engine, constructed the land uplift animation, and wrote the first draft of the manuscript. Ville Mäkinen contributed to developing the land uplift model. Hando-Laur Habicht contributed to the data pre-processing and modeling. Juha Oksanen created the original research idea, planned the study, and developed the initial modeling method for paleotopographic reconstructions. The authors together wrote and revised the paper.

Declaration of competing interest

The authors declare that they have no known competing financial interests or personal relationships that could have appeared to influence the work reported in this paper.

Acknowledgments

This study was conducted as part of the *Lystra* project, which received funding from Interreg Botnia-Atlantica.

We used computing resources provided by the Open Geospatial Information Infrastructure for Research (oGIIR, urn:nbn:fi:research-infras-2016072513) funded by the Academy of Finland.

We are grateful to Dr. Maaria Nordman (Finnish Geospatial Research Institute FGI, National Land Survey of Finland) for valuable advice and help with land uplift and ice sheet modeling.

References

Berglund, M., 2004. Holocene shore displacement and chronology in Ångermanland, eastern Sweden, the Scandianvian glacio-isostatic uplift centre. Boreas 33 (1), 48–60. https://doi.org/10.1080/03009480310006961.

Church, J.A., Clark, P.U., Cazenave, A., Gregory, J.M., Jevrejeva, S., Levermann, A., Merrifield, M.A., Milne, G.A., Nerem, R.S., Nunn, P.D., Payne, A.J., Pfeffer, W.T., Stammer, D., Unnikrishnan, A.S., 2013. Sea level change. In: Stocker, T.F., Qin, D., Plattner, G.-K., Tignor, M., Allen, S.K., Boschung, J., Nauels, A., Xia, Y., Bex, V., Midgley, P.M. (Eds.), Climate Change 2013: the Physical Science Basis. Contribution of Working Group I to the Fifth Assessment Report of the Intergovernmental Panel on Climate Change. Cambridge University Press, Cambridge, United Kingdom and New York, NY, USA.

Danzeglocke, U., Jois, O., Wenninger, B., 2008. CalPal 2007 Online. http://www.calpal-online.de/.

DiBiase, D., MacEachren, A.M., Krygier, J.B., Reeves, C., 1992. Animation and the role of map design in scientific visualization. Cartogr. Geogr. Inf. Syst. 19 (4), 201–214.

Dorling, D., 1992. Stretching space and splicing time: from cartographic animation to interactive visualization. Cartogr. Geogr. Inf. Syst. 19 (4), 215–227.

Ekman, M., 2001. Computation of historical shore levels in Fennoscandia due to postglacial rebound. Small Publ. Hist. Geophys. 8, 14.

Ekman, M., 2017. Calculation of Historical Shore Levels Back to 500 A.D. in the Baltic Sea Area due to Postglacial Rebound. Summer Institute for Historical Geophysics, Åland Islands.

Eronen, M., Haila, H., 1992. The main ancient shorelines. In: Alalammi, P. (Ed.), Atlas of Finland, Folio 123–126: Geology. National Board of Survey & Geographical Society of Finland, Helsinki, p. 17.

Eronen, M., 2005. Land uplift: virgin land from the sea. In: Seppälä, M. (Ed.), The Physical Geography of Fennoscandia: 17-34. Oxford University Press, Oxford.

Howat, I.M., Porter, C., Smith, B.E., Noh, M.-J., Morin, P., 2019. The reference elevation model of Antarctica. Cryosphere 13, 665–674. https://doi.org/10.5194/tc-13-665-2019.

Johansson, M.M., Pellikka, H., Kahma, K.K., Ruosteenoja, K., 2012. Global sea level rise scenarios adapted to the Finnish coast. J. Mar. Syst.

Leverington, D., Teller, J., Mann, J., 2002. A GIS method for reconstruction of late Quaternary landscapes from isobase data and modern topography. Comput. Geosci. 28, 631–639. https://doi.org/10.1016/S0098-3004(01)00097-8.

Lindén, P., Möller, S., Björck, P., Sandgren, 2008. Holocene shore displacement and deglaciation chronology in Norrbotten, Sweden. Boreas 35 (2006), 1–22.

Mäkiaho, J.-P., 2009. Helsinki - itämeren tytär: Paikkatietomenetelmät rannansiirtymistutkimuksessa. Terra 121 (1), 3–17.

Michael Lewis, C.F., Blasco, S., Gareau, P., 2005. Glacial isostatic adjustment of the Laurentian Great Lakes basin: using the empirical record of strandline deformation for reconstruction of early Holocene paleo-lakes and discovery of a hydrologically closed phase. Géogr. Phys. Quaternaire 59 (2–3), 187–210.

Muru, M., Rosentau, A., Preusser, F., Plado, J., Sibul, I., Joeleht, A., Kriiska, A., 2018. Reconstructing Holocene shore displacement and stone age palaeogeography from a foredune sequence on Ruhnu island, gulf of Riga, Baltic Sea. Geomorphology 303, 434–445. https://doi.org/10.1016/j.geomorph.2017.12.016.

Nirgi, T., Rosentau, A., Habicht, H.-L., Hang, T., Jonuks, T., Jõeleht, A., Tõnisson, H., 2019. Holocene Relative Shore-Level Changes and Stone Age Palaeogeography of the Pärnu Bay Area, Eastern Baltic Sea. The Holocene. Epub ahead of print. https://doi.org/10.1177/0959683619865603.

Nordman, M., Milne, G., Tarasov, L., 2015. Reappraisal of the Angerman River decay time estimate and its application to determine uncertainty in Earth viscosity structure. Geophys. J. Int. 201 https://doi.org/10.1093/gji/ggv051.

Ojala, A., Palmu, J.-P., Åberg, A., Åberg, S., Virkki, H., 2013. Development of an ancient shoreline database to reconstruct the Litorina Sea maximum extension and the highest shoreline of the Baltic Sea basin in Finland. Bull. Geol. Soc. Finland 85, 127–144. https://doi.org/10.17741/bgsf/85.2.002.

Oksanen, J., 2012. Land Uplift in North Ostrobothnia between -5000 – 2000. https://www.youtube.com/watch?v=Y753x2Xb4gY.

Påsse, T., Andersson, L., 2005. Shore-level displacement in Fennoscandia calculated from empirical data. GFF 127 (4), 253–268.

Poutanen, M., Steffen, H., 2015. Land uplift at kvarken archipelago/high coast UNESCO world heritage area. Geophysica 50, 49–64.

Rosentau, A., Veski, S., Kriiska, A., Aunap, R., Vassiljev, J., Saarse, L., Hang, T., Heinsalu, A., Oja, T., 2011. Palaeogeographic Model for the SW Estonian Coastal Zone of the Baltic Sea. https://doi.org/10.1007/978-3-642-17220-5_8.

Saaranen, V., Lehmuskoski, P., Rouhiainen, P., Takalo, M., Mäkinen, J., Poutanen, M., 2009. The New Finnish Height Reference N2000, vol. 134. International Association of Geodesy Symposia. https://doi.org/10.1007/978-3-642-00860-3_46.

Stroeven, A.P., Hättestrand, C., Kleman, J., Heyman, J., Fabel, D., Fredin, O., Goodfellow, B.W., Harbor, J.M., Jansen, J.D., Olsen, L., Caffee, M.W., Fink, D., Lundqvist, J., Rosqvist, G.C., Strömberg, B., Jansson, K.N., 2016. Deglaciation of Fennoscandia. Quat. Sci. Rev. 147, 91–121. https://doi.org/10.1016/j.quascirev.2015.09.016.

Tikkanen, M., Oksanen, J., 2002. Late Weichselian and Holocene shore displacement history of the Baltic Sea in Finland. Fennia - Int. J. Geogr. 180 (1–2), 9–20.

United Nations Educational, Scientific and Cultural Organization (UNESCO), 2006. Extension of Properties Inscribed on the World Heritage List (Kvarken Archipelago/High Coast). 30th Session of the World Heritage Committee (30 COM). Vilnius, Lithuania.

Walcott, R.I., 1980. Rheological models and observational data of glacio-isostatic rebound. In: Morner, N.-A. (Ed.), Earth Rheology, Isostasy and Eustasy. John Wiley, pp. 3–10.